WALAILAK JOURNAL

http://wjst.wu.ac.th Engineering and Physical Sciences

Thermal Efficiency of a New Prototype of Evacuated Tube Collector using Sn-Al_2O_3 as a Selective Solar Absorber

Warisa WAMAE[1], Tawat SURIWONG[1,*] and
Thotsaphon THRERUJIRAPAPONG[2]

[1]School of Renewable Energy and Smart Grid Technology, Naresuan University,
Phitsanulok 65000, Thailand
[2]Department of Materials and Production Technology Engineering, Faculty of Engineering,
King Mongkut's University of Technology North Bangkok, Bangkok 10800, Thailand

([*]Corresponding author's e-mail: tawats@nu.ac.th)

Received: 31 October 2017, Revised: 23 January 2018, Accepted: 5 March 2018

Abstract

Three tin pigmented aluminium oxide (Sn-Al_2O_3) films were prepared with different tin content using an anodization process, which is applied as a selective solar absorber in a new prototype of evacuated tube collector (ETC). The morphology and distribution of elements on the coatings were characterized using a Scanning Electron Microscope (SEM) equipped with an Energy Dispersive X-ray (EDX) analyzer. The spectrally selective properties, defined as the ratio of solar absorptance (α_{sol}) to thermal emittance (ε_{therm}) were examined. In order to investigate the thermal performance of ETC using Sn-Al_2O_3 on an Al fin as a solar receiver, thermal efficiency (η) of the ETC was collected under steady-state conditions, as prescribed by ISO 9806-1 standard. The results, of the Sn-Al_2O_3 coatings reached a darker black colour with an increase in the colouring time. The samples were composed of different contents of Sn in the Al_2O_3 layer. The solar selectivity ($\alpha_{sol}/\varepsilon_{therm}$) significantly increased with the increases in Sn content. The maximum thermal efficiency (η_{max}) of the ETC under the nearly constant heat loss coefficient (U_L), was obviously increased with the increasing Sn content. Therefore, the Sn-Al_2O_3 with different Sn contents is a good candidate for selective solar absorbers in a new prototype of ETC.

Keywords: Evacuated tube collector, Selective solar absorber, Anodization, Absorptance, Thermal emittance

Introduction

The normal selective solar absorber coating is coated on the surface of the inner glass tube as in **Figures 1a** and **1b**), which is applied using high technology and a complicated process, which causes high production costs. During the applications, it was found that it is inclined to crack or splits which means that it needs to be replaced, thus causing extra dissipation costs. A changing of solar absorber coating on an aluminium (Al) fin and inserting it into a transparent evacuated tube were developed as a new prototype of ETC (see **Figures 1c** and **1d**). The thermal efficiency and potential for energy production are similar to commercially available ETC's [1].

Selected papers from The 1st MRS Thailand Conference, October 31st - November 3rd, 2017

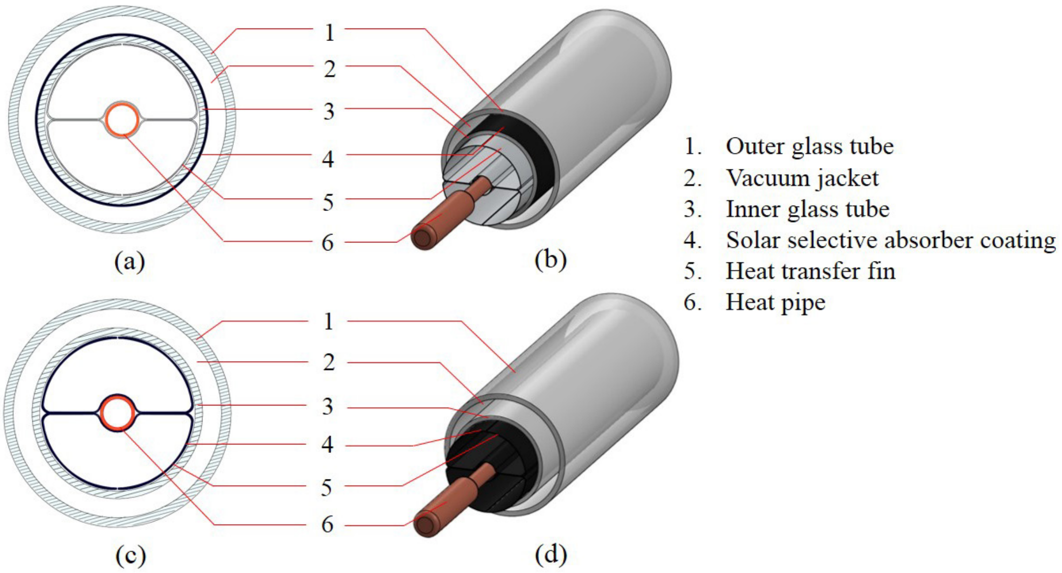

Figure 1 Cross-sectional images of the evacuated tube collector; (a, b) original coating and (c, d) Sn-Al_2O_3 coating on Al fins.

The selective spectral properties of a solar absorber can be enhanced by an appropriate choice of substrate and antireflection layers, which can also protect its surface [2]. Cermet coatings of fine metal particles in a dielectric or ceramic matrix, a good candidate for solar absorber materials at high temperatures, have been successfully commercialized [2,3]. Metal pigmented-Al_2O_3 solar absorbers were prepared by an anodization process; one of the cermet solar absorber coatings. It is well known that anodization is a simple technique in the aluminium coating industry that satisfies each of these factors to produce a high-performance aluminium finish, which can have an extremely long lifetime and offer significant economic advantages through maintenance and operational savings. For the improvement of the selective solar absorber properties, there are several black pigments which are applied on the aluminum oxide film, such as W-Al_2O_3 cermet, Ag-Al_2O_3 nanocermet, Mo-Al_2O_3, Pt-Al_2O_3, Ni-Al_2O_3, Cu-$CuAl_2O_4$ and Si-Al_2O_3 [4-10]. Recently, it was found that tin (Sn) is one of the pigments which is able to deposit into the Al_2O_3 film layer as the cermet (metal-dielectric composite) coating for applying as a solar absorber material in solar thermal applications [11,12]. The α_{sol} of the tin pigmented-Al_2O_3 (Sn-Al_2O_3) increases according to the increase of Sn contents while the thermal conductivity of the Sn–Al_2O_3 samples decreases with increasing Sn content [13]. In addition, the Sn-Al_2O_3 coating prepared by the anodization process has been considered due to an eco-innovative production method for sustainable development. Presently, the applications of Sn-Al_2O_3 coating as solar absorber in solar thermal devices with low and mid-operational temperature range has not been investigated. In the present study, therefore, the influence of Sn content deposited into the Al_2O_3 porous layer on solar selectivity ($\alpha_{sol}/\varepsilon_{therm}$) was determined, together with the morphological characterization of the coatings. The thermal efficiency (η) of the new prototype of ETC using Sn-Al_2O_3 selective solar coatings on an Al fin applied as a solar receiver was investigated.

Materials and methods

The anodized aluminium specimens

The commercial Al fin of 9 cm wide × 160 cm long with a thickness of 0.02 cm was used as the substrate. The Al fin was degreased by a cleaning solution, then etched by NaOH solution, and immersed in 165 g/l H_2SO_4 solution. The anodic anodizing process was conducted in an electrolyte bath containing a lead plate as the cathode (-) and the Al fin was attached to the anode (+). A direct current electrical supply of 1,000 A at 15-17 V was applied for 45 minutes to achieve a translucent Al_2O_3 film on the surface of Al fin by controlling the electrolyte temperature at 20 °C. Then, the anodized Al fin was transferred to the coloring bath containing the tin (II) sulphate ($SnSO_4$). In this process, the deposition of tin pigmentation into the pore of translucent Al_2O_3 film (Sn-Al_2O_3) was carried out for 5, 7 and 10 min, which coded as Sn-Al_2O_3-5, Sn-Al_2O_3-7 and Sn-Al_2O_3-10, respectively.

Characterization of anodized aluminium coatings

The elemental distribution profile of all coating samples was characterized by a Low Vacuum Scanning electron microscope equipped with an Energy dispersive X-ray analyzer (LV-SEM-EDX, JSM-5910 JEOL). The α_{sol} of the Sn-Al_2O_3 with different Sn contents was calculated based on the relationship of the measured spectral reflectance (R) in the wavelength range of 0.3 - 2.5 µm from an ultraviolet-visible-near infrared spectrophotometer (Shimadzu UV-3101PC). While the ε_{therm} at 100 °C was calculated from the R in the infrared region (2.5 - 25 µm) obtained by the Fourier transform infrared spectrophotometer result (FTIR, Bruker Tensor 27), and compared to the Planck blackbody distribution at the specific temperature as following equations [14];

$$\alpha_{sol} = \frac{\int_{0.3\mu m}^{2.5\mu m} I_s(\lambda)(1-R(\lambda))d\lambda}{\int_{0.3\mu m}^{2.5\mu m} I_s(\lambda)d\lambda} \tag{1}$$

$$\varepsilon_{therm} = \frac{\int_{2.5\mu m}^{25\mu m} I_b(\lambda)(1-R(\lambda))d\lambda}{\int_{2.5\mu m}^{25\mu m} I_b(\lambda)d\lambda} \tag{2}$$

where $I_s(\lambda)$ is the solar spectral irradiance at AM 1.5, $R(\lambda)$ is the spectral reflectance, and $I_b(\lambda)$ is the spectral blackbody emissive power at room temperature. The solar selectivity of the selective solar absorber is defined as the proportion of the solar absorptance (α_{sol}) and thermal emittance (ε_{therm}), indicating that the $\alpha_{sol}/\varepsilon_{therm}$ means the efficiency of solar absorber materials.

Thermal efficiency test

The Sn-Al_2O_3 selective solar absorber coated on Al fin was assembled with a heat pipe and transparent double layer borosilicate evacuated tube as one set of solar receiver tubes. Then, the new prototype of ETC was obtained by using 15 tubes of solar receiver tube sets mounted with a header and manifold. The thermal efficiency test of the ETC was measured under steady-state conditions as prescribed by the ISO 9806-1 standard. The assembly of the thermal efficiency test system is shown in **Figure 2**. The collector area is 1.08 m^2. The parameters for the thermal efficiency test consists of ambient temperature (T_a), fluid mass flow rate ($\dot{m}$) and global solar irradiance (G_t) at the collector plane, as summarized in **Table 1**. The inlet temperature (T_i) was controlled to be at 30, 40, 50 and 60 °C, while the outlet temperature (T_o) was collected. The thermal efficiency (η) was calculated by the first-degree equation (linear regression);

$$\eta = \frac{\dot{m}c_p(T_o - T_i)}{A_a G_t} \tag{3}$$

$$\eta = F_R(\tau\alpha) - F_R U_L \left(\frac{T_i - T_a}{G_t} \right) \tag{4}$$

where c_p is specific heat capacity, A_a is the gross collector aperture area, F_R is the heat removal factor which is defined as the actual useful energy gain of ETC to the useful gain, τ is the transmittance of transparent double layer borosilicate evacuated tube ($\tau = 0.90$) double layer evacuated tube, and U_L is overall heat loss coefficient. A thermal efficiency equation was performed with a convenient mathematical tool of a linear least-squares fit established with 50 data points/sample.

Figure 2 Thermal efficiency testing system at School of Renewable Energy Technology, Naresuan University, Thailand (Latitude 16°44′ N and Longitude 100°11′ E).

Table 1 Parameters for the thermal efficiency test.

Parameters	Factors
Solar irradiance (G_t)	800 ± 50 W/m^2
Ambient or surrounding air temperature (T_a)	29 - 31 °C
Fluid mass flow rate ($\dot{m}$)	0.216 kg/s, ± 1 %
Fluid temperature at the collector inlet (T_i)	30 - 60 °C, ± 0.1 °C

Results and discussion

The Sn-Al$_2$O$_3$ coating on Al fin with variation of time in the coloring bath was successfully prepared by anodic anodization, as shown in **Figure 3**. It was observed that the coatings reached to darker black with increasing the coloring time. The Sn-Al$_2$O$_3$-5 was dark brown, the Sn-Al$_2$O$_3$-7 was black and brown and the Sn-Al$_2$O$_3$-10 was dark black.

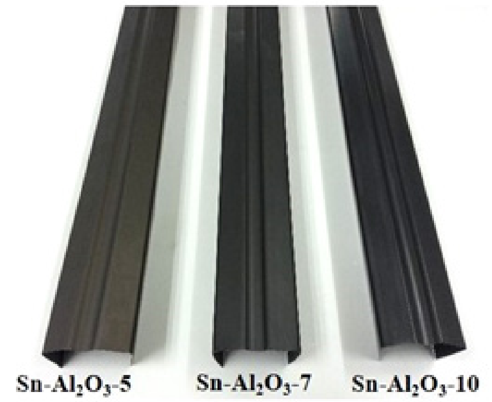

Figure 3 Sn-Al$_2$O$_3$ coatings on Al fin with variation of coloring time.

Figure 4 presents the elemental distribution profiles in the cross-section of the Sn-Al$_2$O$_3$ coatings on Al fin samples which characterized by SEM-EDX with the line scan analysis. The translucent Al$_2$O$_3$ film of all samples was the identical thickness of 9.1 - 9.5 μm due to the same of anodization time during the anodic oxidation process. It is indicated that the coating samples consist of 2 layers; a compact Al$_2$O$_3$ barrier layer close to the interface of Al substrate and a porous Al$_2$O$_3$ layer. The Al, O and Sn elements were found in all coatings. The highest content of Al was found at the Al substrate, the content immediately decreased at the interface between the Al$_2$O$_3$ layer and Al substrate, and kept relatively constant through the oxide film layer. The O exhibited the larger content in the Al$_2$O$_3$ film in all the samples, indicating that Al$_2$O$_3$ was formed by anodic anodization. The SEM images of all the samples present 2 different contrast areas with a strong chemical composition contrast in the Al$_2$O$_3$ layer as a result of the different atomic number of elements. The light grey area was the Sn pigment rich area which exhibited a high content near the Al substrate interface of the Al fin. The Sn impregnated into the pores of Al$_2$O$_3$ appeared like the spike shape, according to Ni-Al$_2$O$_3$ prepared by the anodization technique [15-17]. The length of spike shape or Sn pigment rich area increased with increasing the coloring time in the order Sn-Al$_2$O$_3$-5 < Sn-Al$_2$O$_3$-7 < Sn-Al$_2$O$_3$-10. As shown in **Figure 4**, the Al$_2$O$_3$ layer for all samples was controlled to an identical thickness, while the increasing amount of Sn into the pores of Al$_2$O$_3$ layer lead to an increasing size and length of the spike-like Sn layer. This is due to the increasing time for electrochemical deposition in coloring process leading to increasing the Sn content deposited into the pores of Al$_2$O$_3$. The phase structure of Sn-Al$_2$O$_3$ of all coatings was not changed with increasing the coloring time.

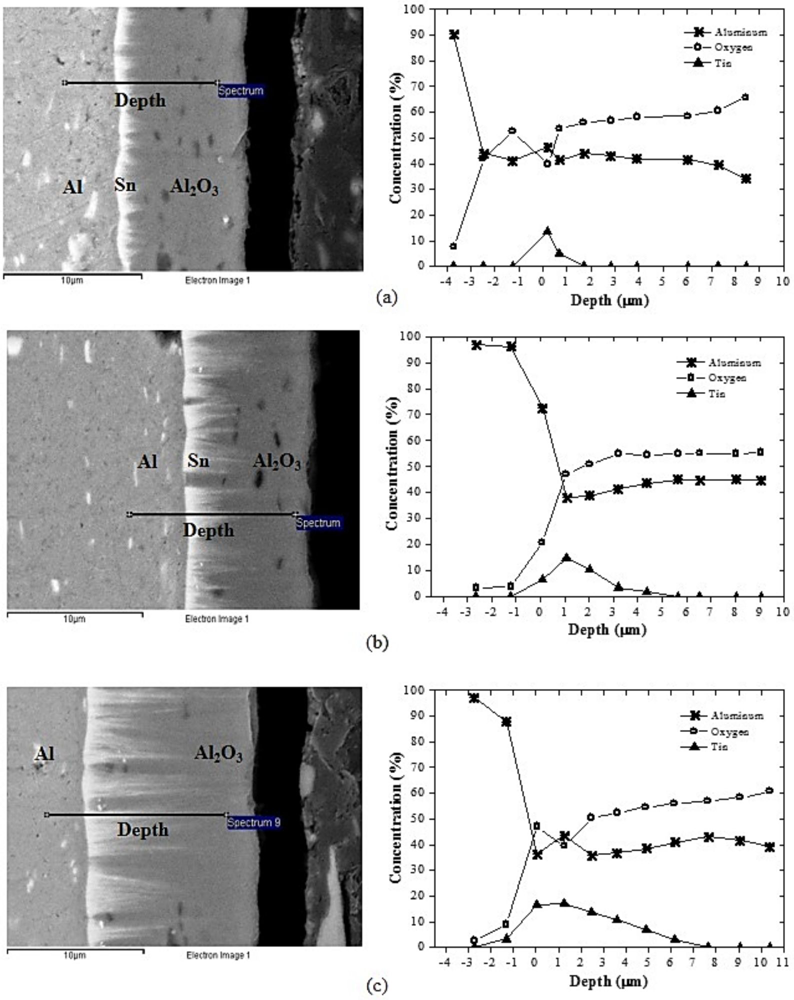

Figure 4 SEM-EDX line scanning profiles and chemical compositions of (a) Sn-Al_2O_3-5, (b) Sn-Al_2O_3-7 and (c) Sn-Al_2O_3-10.

According to the theoretical properties to achieve a high performance of selective solar absorber, the coatings require a high α_{sol} ($\alpha_{sol} \approx 1$) or low R ($R \approx 0$) in the solar spectrum region ($0.3 < \lambda \leq 3$ µm) and low ε_{therm} ($\varepsilon_{therm} \approx 0$) or high R ($R \approx 1$) in the infrared region ($\lambda \geq 3$ µm) at the operational temperature of the solar thermal applications [2]. As the cermet selective solar absorbers, ceramic matrix or dielectric layers increase the absorption in the UV-VIS regions, and metal layers and a highly IR-reflective metal substrate effectively increase the R in the IR region [3]. **Figure 5a** presents the measured R of all the Sn-Al_2O_3 coatings in the UV-Vis-NIR region, according to the whole wavelength interval of the solar spectrum at AM 1.5 (0.3 - 2.5 µm). It is found that the R of all samples was relatively low in the whole wavelength range. With increasing the wavelength, the R of all samples was gradually increased and rather high in the near infrared region. The α_{sol} of all samples was calculated by Eq. (1) and shown in **Figure 5a**. The α_{sol} significantly increased with increasing the Sn content in the Al_2O_3 layer. This is due to more light scattering because of the Sn particles inside the Al_2O_3 pores. The light scatter caused more solar radiation to be trapped in the absorber materials [2,15]. In addition, the transparent Al_2O_3 layer plays an important role in the anti-reflection layer, obstructing the reflection of solar radiation from the Sn particles, as a result of the reflective index mismatch between air and the Sn-Al_2O_3 layer. Compared to previous studies, the α_{sol} of the present study was slightly greater than that of several black coatings on the Al substrate [6-8], including the CuO coating on anodized Al, α_{sol} = 0.85 [18]. Especially, the α_{sol} of Sn-Al_2O_3-10 sample was close to that of the Black Ni-Co on Al alloy, α_{sol} = 0.95 [19]. So, the Sn content in the Sn-Al_2O_3 coatings has a significant effect in improving α_{sol}. **Figure 5b** presents the measured R of all the samples in the wavelength range of IR region. The R of all the samples was above 95 % ($R > 0.95$) as in the wavelength range of 2.5 - 8.0 μm, then gradually decreased. It is indicated that the long-wavelength radiation is reflected and scattered back by the Sn layers and the Al substrate [3]. However, the Sn-Al_2O_3-7 coating exhibited the highest spectral R, corresponding with the increased R in the IR region by adding more particles with a small film thickness of Al_2O_3 [2,14]. The ε_{therm} was calculated based on the Planck blackbody distribution at 100 °C. The ε_{therm} of all samples was relatively different in the range of 0.21 - 0.24. It is implied that increasing the Sn content into the pores of the Al_2O_3 layer has little effect on the ε_{therm} of the Sn-Al_2O_3 coatings, in good agreement with the increasing emissivity of the anodic oxide coating on the Al substrate with the thickening of the oxide film as a result of the different microstructure in the oxide film [20]. When compared to previous studies, the ε_{therm} of all samples close to the Mo-Al_2O_3 (ε_{therm} = 0.19) [6], and Ni-Al_2O_3 coatings (ε_{therm} = 0.22) [8].

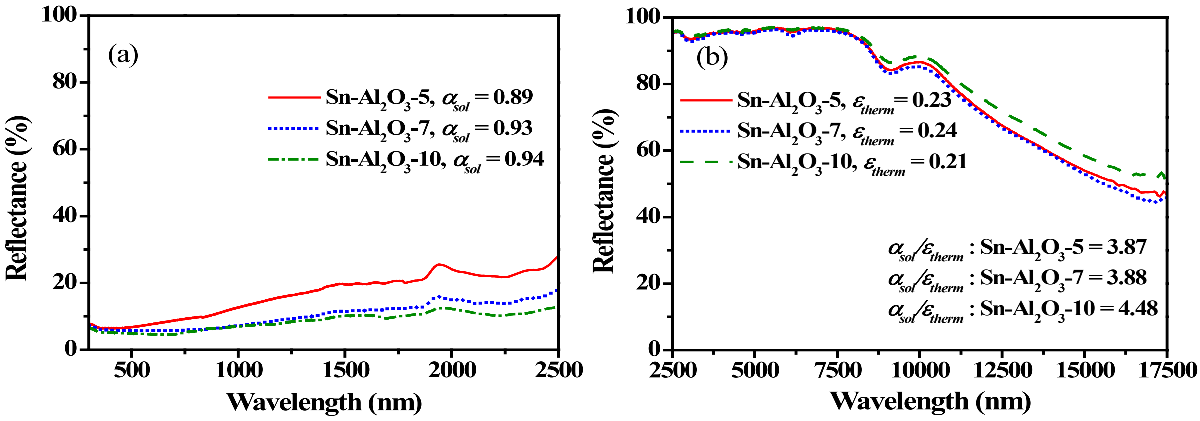

Figure 5 Spectral reflectance (R) measurement of Sn-Al_2O_3 coatings on Al fin with different Sn contents in the wavelength range of (a) UV-Vis-NIR and (b) the IR region.

As shown in **Figure 5**, the characteristic spectral R of all Sn-Al_2O_3 samples exhibits the behavior similar to the theoretical properties of spectral selective solar absorber. To consider the morphology of the segregated Sn at the interface, the α_{sol} is dependent on the morphology (spike size and length) of spike-like Sn layer, while the ε_{therm} has little effect. In order to discuss on the spectral solar selectivity of the Sn-Al_2O_3 solar absorber materials in more detail, the solar selectivity ($\alpha_{sol}/\varepsilon_{therm}$) of the samples should be evaluated. Although there is no theoretical limit for the maximum $\alpha_{sol}/\varepsilon_{therm}$, in order to maximize the $\alpha_{sol}/\varepsilon_{therm}$ of solar absorber materials, the α_{sol} is required to be at the highest, but ε_{therm} should be reduced as much as possible. The $\alpha_{sol}/\varepsilon_{therm}$ of the samples are summarized in **Figure 5b**. The $\alpha_{sol}/\varepsilon_{therm}$ of the Sn-Al_2O_3 samples were 3.87 - 4.48. With increasing the Sn content, the $\alpha_{sol}/\varepsilon_{therm}$ of the Sn-Al_2O_3 coatings increased. The $\alpha_{sol}/\varepsilon_{therm}$ of the coatings was relatively lower than that of the related coatings prepared using various sputtering techniques such as Ag-Al_2O_3 [5], AlNi-Al_2O_3 [21], Pt-Al_2O_3 [22] and Al_2O_3-WC [23]. The $\alpha_{sol}/\varepsilon_{therm}$ of Sn-Al_2O_3-10 sample is close to that of the Mo-Al_2O_3 ($\alpha_{sol}/\varepsilon_{therm}$ = 4.84) deposited by magnetron sputtering technique [6], and the Ni-Al_2O_3 coating ($\alpha_{sol}/\varepsilon_{therm}$ = 4.41 - 8.36) prepared using anodization process [8].

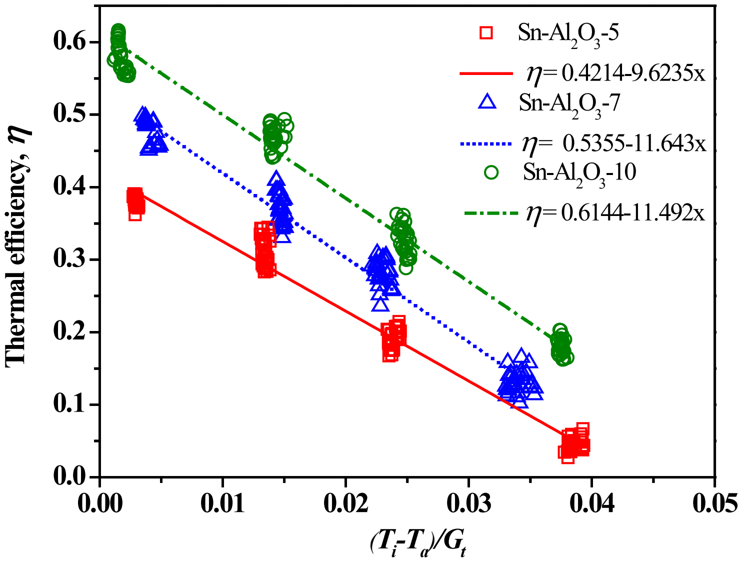

Figure 6 The thermal performance curve of the new prototype ETC using (a) Sn-Al$_2$O$_3$-5, (b) Sn-Al$_2$O$_3$-7 and (c) Sn- Al$_2$O$_3$-10 as a selective solar absorber.

The Sn-Al$_2$O$_3$ with different Sn contents were applied as selective solar absorbers in the new prototype of ETC. According to the collected data from the thermal efficiency testing system, the η were calculated by Eq. 3 and 4. The thermal performance curve, of η verses $(T_i-T_a)/G_t$, was plotted, as shown in **Figure 6**. To consider the thermal efficiency equations, the interception on the vertical efficiency, F_R $(\tau\alpha)$, was 0.42, 0.54, and 0.61 for the Sn-Al$_2$O$_3$-5, Sn-Al$_2$O$_3$-7 and Sn-Al$_2$O$_3$-10, respectively. While, the slope ($-F_RU_L$), which is defined as no useful energy, was -9.62, -11.64 and -11.49 W/m^2·°C for the Sn-Al$_2$O$_3$-5, Sn-Al$_2$O$_3$-7 and Sn-Al$_2$O$_3$-10, respectively.

In order to consider the influence of different Sn content impregnated Sn-Al$_2$O$_3$ selective solar absorbers on the thermal performance of ETC, the parameters related to the thermal efficiency equation should be performed. **Table 2** presents the summary of the thermal performance parameters of ETC using Sn-Al$_2$O$_3$ selective solar absorbers. It is clearly observed that not only the F_R increase with increasing the Sn content into the pores of Al$_2$O$_3$, but also the U_L decrease. The F_R increased with increasing Sn content, indicating that the actual useful energy gain of the new prototype ETC also increased. It implies the solar radiation is directly converted to thermal energy at the Sn-Al$_2$O$_3$ solar absorbers, after that useful heat is easily transferred through the Al fin and exchanger, respectively. According to the $\alpha_{sol}/\varepsilon_{therm}$ of Sn-Al$_2$O$_3$ coatings, the U_L of the new prototype of ETC decreased with the increasing amount of Sn. Among the thermal performance testing, the new prototype ETC using the Sn-Al$_2$O$_3$-10 solar absorber exhibits the highest thermal performance. It is clearly seen, that the higher Sn content into the Al$_2$O$_3$ porous layer leads to enhancing the thermal performance of the new prototype ETC as a result of increasing F_R, together with decreasing the U_L.

However, the thermal performance curve of the ETC prototype using Sn-Al$_2$O$_3$ with different Sn content over an Al fin as solar absorber was slightly lower than in previous studies with several approaches for enhancing the thermal performance [24,25]. So, the new prototypes of ETC with changing the position of the solar absorber from the inner double glass tube to Al fin coated with the Sn-Al$_2$O$_3$ selective solar absorber is considered as a good competitor to commercially available solar collectors, indicating that the role of the Al fin is a solar receiver and heat transfer medium at the same time.

Table 2 Summary of thermal performance parameters of the new ETC prototype using Sn-Al_2O_3 as a selective solar absorber.

Samples	$\eta = F_R(\tau\alpha) - F_R U_L\left(\frac{T_i - T_a}{G_t}\right)$	$F_R(\tau\alpha)$	F_R	U_L	$-F_R U_L$
Sn-Al_2O_3-5	$\eta = 0.4214 - 9.6235x$	0.42	0.52	18.35	-9.62
Sn-Al_2O_3-7	$\eta = 0.5355 - 11.644x$	0.54	0.64	18.04	-11.64
Sn-Al_2O_3-10	$\eta = 0.6144 - 11.492x$	0.61	0.72	15.94	-11.49

Conclusions

The Sn-Al_2O_3 selective solar absorber was successfully prepared as a selective solar absorber by the anodic anodization process with different Sn contents into the pores of the Al_2O_3 layer. The Al, O and Sn distributions were confirmed by SEM-EDX with the line scan technique. The Sn impregnated into the pores of Al_2O_3 appeared in a spike shape, and exhibited a high content near the Al substrate interface of the Al fin. The length of the spike shape or Sn pigment rich area increased with increasing the coloring time in the electrochemical deposition process. The $\alpha_{sol}/\varepsilon_{therm}$ of the Sn-Al_2O_3 coatings increased with increasing the Sn content. As the results of the thermal performance curve of the new ETC prototype, the higher Sn content into the pores of Al_2O_3 leads to the enhancement of the thermal performance of the new prototype ETC as the result of increasing F_R, together with decreasing U_L. Therefore, the new prototype of ETC using the Sn-Al_2O_3 selective solar absorber is considered as a good competitor to commercial solar collectors, indicating the role of the Al fin is a solar receiver and heat transfer medium at the same time. Also, it is a guideline for enhancing thermal performance and developing the new eco-innovative ETC prototype.

Acknowledgements

The authors gratefully acknowledge to The Thailand’s Office of the Higher Education Commission, Thailand for giving the scholarship in the Ph.D. program (Renewable energy) to Miss Warisa Wamae (Contract no. 026/2556). Also, we are grateful to the National Research Council of Thailand (NRCT), through Naresuan University, for providing financial support (Grant no. R2561B107).

References

[1] P Nunocha, T Suriwong and T Threrujirapapong. Development and application of anodized aluminium for selective absorber in evacuated tube collector (ETC). *Naresuan Univ. J. Sci. Tech.* 2014; **22**, 75-84.

[2] CE Kennedy. *Review of Mid-to High-Temperature Solar Selective Absorber Materials*. National Renewable Energy Laboratory, Colorado, 2002.

[3] P Bermel, J Lee, JD Joannopoulos, I Celanovic and M Soljačiç. Selective solar absorbers. *Annu. Rev. Heat Trans*. 2012; **20**, 231-54.

[4] A Antonaia, A Castaldo, ML Addonizio and S Esposito. Stability of W-Al_2O_3 cermet based solar coating for receiver tube operating at high temperature. *Sol. Energ. Mater. Sol. Cells* 2010; **94**, 1604-11.

[5] HC Barshilia, P Kumar, KS Rajam and A Biswas. Structure and optical properties of Ag–Al_2O_3 nanocermet solar selective coatings prepared using unbalanced magnetron sputtering. *Sol. Energ. Mater. Sol. Cells* 2011; **95**, 1707-15.

[6] D Xinkang, W Cong, W Tianmin, Z Long, C Buliang and R Ning. Microstructure and spectral selectivity of Mo–Al_2O_3 solar selective absorbing coatings after annealing. *Thin Solid Films* 2008; **516**, 3971-7.

[7] TK Vien, C Sella, J Lafait and S Berthier. Pt-Al_2O_3 selective cermet coatings on superalloy substrates for photothermal conversion up to 600°C. *Thin Solid Films* 1985; **126**, 17-22.

[8] A Wazwaz, J Salmi, H Hallak, and R Bes. Solar thermal performance of a nickel-pigmented aluminium oxide selective absorber. *Renew. Energy* 2002; **27**, 277-292.

[9] D Ding, W Cai, M Long, H Wu and Y Wu. Optical, structural and thermal characteristics of Cu–$CuAl_2O_4$ hybrids deposited in anodic aluminum oxide as selective solar absorber. *Sol. Energ. Mater. Sol. Cells* 2010; **94**, 1578-81.

[10] V Naumann, M Otto, RB Wehrspohn, M Werner and C Hagendorf. Interface and material characterization of thin ALD-Al_2O_3 layers on crystalline silicon. *Energ. Proc.* 2012; **27**, 312-8.

[11] MF Shaffei, N Khattab, AM Awad and HS Hussein. Characterization of black Ni and Sn as optically selective absorber coatings in thermal solar collectors mainly (Part I). *Res. J. Pharm. Biol. Chem. Sci.* 2014; **5**, 173-82.

[12] T Chorchong, T Suriwong, S Sukchai and T Threrujirapapong. Characterization and spectral selectivity of Sn-Al_2O_3 solar absorber. *Key Eng. Mater.* 2015; **675-676**, 467-72.

[13] W Wamae, T Suriwong and T Threrujirapapong. Influence of tin content on spectral selectivity and thermal conductivity of Sn–Al_2O_3 solar selective absorber. *Materials for Renewable and Sustainable Energy*, 2018; **7**, 1-8.

[14] T Tesfamichael. 2000, Characterization of Selective Solar Absorbers, Ph.D. Dissertation. Uppsala University, Uppsala, Sweden.

[15] A Wazwaz, J Salmi and R Bes. The effects of nickel-pigmented aluminium oxide selective coating over aluminium alloy on the optical properties and thermal efficiency of the selective absorber prepared by alternate and reverse periodic plating technique. *Energ.Convers. Manag.* 2010; **51**, 1679-83.

[16] A Andersson, O Hunderi and CG Granqvist. Nickel pigmented anodic aluminum oxide for selective absorption of solar energy. *J. Appl. Phys.* 1980; **51**, 754-64.

[17] M Bagheri, F Ashrafizadeh and MH Najafabadi. Black nickel coating and color anodized layers for solar absorber. *Trans. Indian Inst. Met.* 2014; **67**, 927-34.

[18] BJ Prakash, B Vishnuprasad and VV Ramana. Performance study on effect of nano coatings on liquid flat plate collector: An experimental approach. *Int. J. Mech. Eng. Rob. Res.* 2013; **2**, 379-84.

[19] AR Shashikala, AK Sharma and DR Bhandari. Solar selective black nickel-cobalt coatings on aluminum alloys. *Sol. Energ. Mater. Sol. Cells* 2007; **91**, 629-35.

[20] T Pavlovic and A Ignatiev. Optical and microstructural properties of anodically oxidized aluminum. *Thin Solid Films* 1986; **138**, 97-109.

[21] Y Xue, C Wang, W Wang, Y Liu, Y Wu, Y Ning and Y Sun. Spectral properties and thermal stability of solar selective absorbing AlNi–Al_2O_3 cermet coating. *Sol. Energ.* 2013; **96**, 113-8.

[22] ZY Nuru, DE Motaung, K Kaviyarasu and M Maaza. Optimization and preparation of Pt–Al_2O_3 double cermet as selective solar absorber coatings. *J. Alloys Compd.* 2016; **664**, 161-8.

[23] XH Gao, CB Wang, ZM Guo, QF Geng, W Theiss and G Liu. Structure, optical properties and thermal stability of Al_2O_3-WC nanocomposite ceramic spectrally selective solar absorbers. *Opt. Mater*. 2016; **58**, 219-25.

[24] L Ma, Z Lu, J Zhang and R Liang. Thermal performance analysis of the glass evacuated tube solar collector with U-tube. *Build. Environ.* 2010; **45**, 1959-67.

[25] E Zambolin and DD Col. Experimental analysis of thermal performance of flat plate and evacuated tube solar collectors in stationary standard and daily conditions. *Sol. Energ.* 2010; **84**, 1382-96.